

Highly-scattering cellulose-based films for radiative cooling

November 30, 2021

Juliana Jaramillo-Fernandez^{A,3,†}, Han Yang^{B,†,}, Lukas Schertel^{B,†}, Guy L. Whitworth^{A,*}, Pedro D. Garcia^{A,2}, Silvia Vignolini^{C,1} and Clivia M. Sotomayor-Torres^{A, C}*

Passive radiative cooling enables the cooling of objects below ambient temperature during daytime without consuming energy, promising to be a game changer in terms of energy savings and CO₂ reduction. However, so far most radiative cooling surfaces are obtained by energy-intensive nanofabrication processes or make use of unsustainable materials. We overcome these limitations by developing cellulose films with unprecedentedly low absorption of solar irradiance and strong mid-IR emittance. In particular, a cellulose derivative (cellulose acetate) was exploited to produce porous scattering films of two different thicknesses, $L \approx 30 \mu\text{m}$ (thin) and $L \approx 300 \mu\text{m}$ (thick), making them adaptable to above and below-ambient cooling applications. The thin and thick films absorb only $\sim 5.2 \%$ and $\sim 5.0 \%$ of the solar irradiance ($\lambda \approx 0.3 - 2.5 \mu\text{m}$), respectively. This low solar absorption represents a gain in net cooling power of at least 17 W/m^2 , compared to state-of-the-art cellulose-based radiative-cooling materials. Field tests show that the films can reach up to $\sim 5 \text{ }^\circ\text{C}$ below ambient temperature, when solar absorption and conductive/convective losses are minimized. Under dryer conditions (water column = 1 mm), we estimate that our films can reach average minimum temperatures of $\sim 7 - 8 \text{ }^\circ\text{C}$ below the ambient. Our work presents an alternative cellulose-based material for efficient radiative cooling that is cost-efficient, simple to fabricate and avoids the use of polluting materials.

1 Introduction

The Earth keeps its thermal equilibrium by dissipating the excess heat from absorbed solar energy to the cold outer space ($\sim 3 \text{ K}$) via thermal radiation. This heat exchange between the planet's surface and outer space takes place because the atmospheric gases barely absorb the outgoing long-wave radiation between 8 and 13 μm . This spectral band, known as the first infra-red (IR) atmospheric transparency

window (IRAW), coincides with the peak wavelength ($9.7 \mu\text{m}$) of black-body radiation at average ambient temperature ($\sim 300 \text{ K}$), enabling the maximization of radiative heat transfer. The same principle applies to all the objects on the Earth's surface. When exposed to the sky, objects radiate the excess heat to outer space through the IRAW^[?,?,?] and exchange heat with the atmosphere at wavelengths where both the objects and atmosphere are opaque. To some extent, the release of heat is damped due to the absorption of the outgoing long-wave radiation by the atmospheric gases at wavelengths outside the IRAW. The absorption by the atmosphere and the consequent radiation of this energy in the infrared (by Kirchhoffs law of thermal radiation)^[?] results in further heating the object at the Earth's surface. Thus, its net radiative heat flux to outer space is limited by the incident thermal radiation from the atmosphere and the absorbed sunlight. Radiative cooling technologies exploit this phenomenon to achieve passive sub-ambient cooling during daytime, and have emerged recently as a promising solution in renewable-energy research.

^A Catalan Institute of Nanoscience and Nanotechnology (ICN2), CSIC and BIST, Campus UAB, Bellaterra, 08193 Barcelona, Spain.

^B Department of Chemistry, University of Cambridge, Lensfield Road, Cambridge.

^C ICREA - Institució Catalana de Recerca i Estudis Avançats, 08010 Barcelona, Spain.

* Current address: School of Chemical Engineering, University of Chinese Academy of Sciences, Beijing 100049, China.

* Current address: The Institute of Photonic Sciences (ICFO), Mediterranean Technology Park, Avinguda Carl Friedrich Gauss, 3, 08860 Castelldefels, Barcelona.

¹e-mail:sv319@cam.ac.uk

²e-mail:david.garcia@icn2.cat

³e-mail:juliana.jaramillo@icn2.cat

[†]These authors contributed equally to this work.

To achieve efficient radiative cooling, the optical properties of materials must be engineered to (i) minimize the absorption of sunlight and atmospheric thermal radiation and (ii) enhance their emittance within the atmospheric transparency window. Many such materials have now been demonstrated using nano- and micro-structured technologies and surface engineering, promising a viable cooling technology for intensive global energy savings that could help mitigating climate change.^[?, ?, ?, ?, ?] For example, remarkable designs include microsphere-based photonic random media,^[?] thin-film multi-layer structures,^[?, ?, ?, ?] microsphere-periodic arrays,^[?, ?] metal-dielectric nanophotonic structures,^[?] double-layer nanoparticle-based coatings,^[?, ?] aerogels,^[?, ?] porous synthetic polymer-based coatings^[?, ?] and hybrid dielectric-polymer materials.^[?, ?, ?, ?] However, several of these technologies come at the cost of demanding engineering and fabrication processes, making difficult their large scale production and therefore their use in real applications. Furthermore, one would ideally exploit sustainable materials to produce such coatings and avoid the use of plastics or heavy metals, to have a meaningful positive impact on the environment. In this context, cellulose derivatives are ideal candidates as they can be produced from cellulose in industrial scale by various chemical modifications.^[?] Specifically, cellulose acetate (AC) is an insoluble cellulose derivative considered as a nontoxic and biodegradable material.^[?, ?] Here, we report on producing highly scattering porous cellulose films for efficient radiative cooling with a scalable production process that does not require any particular or challenging nanostructuring or engineering.

2 Results and discussion

Thin films of cellulose (acetate) with a disordered network morphology where produced by a phase separation method. The achieved porosity enables strong light scattering down to UV wavelengths and across the visible solar spectrum (Fig.2b), while showing thermal emission in the mIR and the IR atmospheric transparency window. We characterize the network morphology, optical transmittance and reflectance spectra as well as their thermal properties to show their applicability and performance for radiative daytime cooling and discuss their potential for sustainable large scale coating applications.

2.1 Tunable thermal and optical properties of radiative cooling films

Passive radiative cooling materials must emit heat to the ultracold-outer space through the IRAW ($\lambda \approx 8 - 13 \mu\text{m}$). Only when the emitted power exceeds the power absorbed by the material over all other wavelengths, the material is able to cool below ambient temperatures. During daytime, achieving temperatures below ambient can be challenging due to heating of

the structures by incident sunlight. The performance of passive-daytime radiative cooling (PDRC) materials with high emittance in the IRAW can be therefore enhanced by designing their morphology to minimize absorption of solar irradiance (i.e reflecting it optimally) over a wide spectral range ($\lambda \approx 0.3 - 2.5 \mu\text{m}$). Such broadband high reflectance is usually easily achieved in thick films of random-network structures through multiple light scattering.^[?] However, this is not trivial in thin films because the light transport mean free path (MFP), which is the length scale on which the orientation of the incoming light is randomized by scattering, is comparable or greater than the film thickness L . On a microscopic length scale, the scattering is limited by the ratio of the film thickness L and the MFP. Thus, achieving high broad-band reflectance in thin-films is difficult as the MFP in non-optimised scattering materials is usually several microns long.^[?]

The thickness of the porous PDRC material is an important design parameter because it not only affects the optical properties but also the thermal performance. Films with larger thickness L can be advantageous to easily achieve strong emittance in the infrared and, at the same time, to provide thermal insulation to minimize parasitic conduction losses. Such characteristics are useful for applications that require cooling below the ambient-temperature (below-ambient cooling). On the other hand, thin structures can be more beneficial for above-ambient cooling, where heat conduction is favorable, e.g when the substrate emits a lot of heat, such as in a generator (Figure 1a).

Here, only using one single approach we produce, via phase-separation, films of cellulose (acetate) with different thicknesses and controlled scattering morphology. We show that the produced thick films ($\approx 300 \mu\text{m}$, filling fraction = 48%) strongly reflect the sunlight and emit in the mid-IR while can also provide thermal insulation to the underlying substrate. On the other hand, the thin films ($\approx 30 \mu\text{m}$, filling fraction = 36%) allow partial transmittance and moderate emittance in the IRAW while still strongly reflecting in the solar spectrum. Fig 1b and Fig 1c show scanning electron micrographs of the films from which the thickness and morphology were characterized (See Experimental section 4 for details).

2.2 Optical characterization

To maximize their cooling effect, we need to engineer the optical properties of radiative-cooling materials over a large spectral range from the UV to the mid-infrared (mid-IR). In figure 2, the optical properties of a thin (black) and a thick (red) film are shown and their emittance is plotted in Figure 2a. For comparison, we also plot the normalized solar irradiance spectrum at air mass (AM) 1.5 (yellow) and the atmospheric transmittance (blue). The features observed in both thick and thin films are very similar over the entire spectral range. A major difference lays in the lower emittance of the thin film around $12 \mu\text{m}$ which is directly associated to a higher transmittance. This could enable the use of

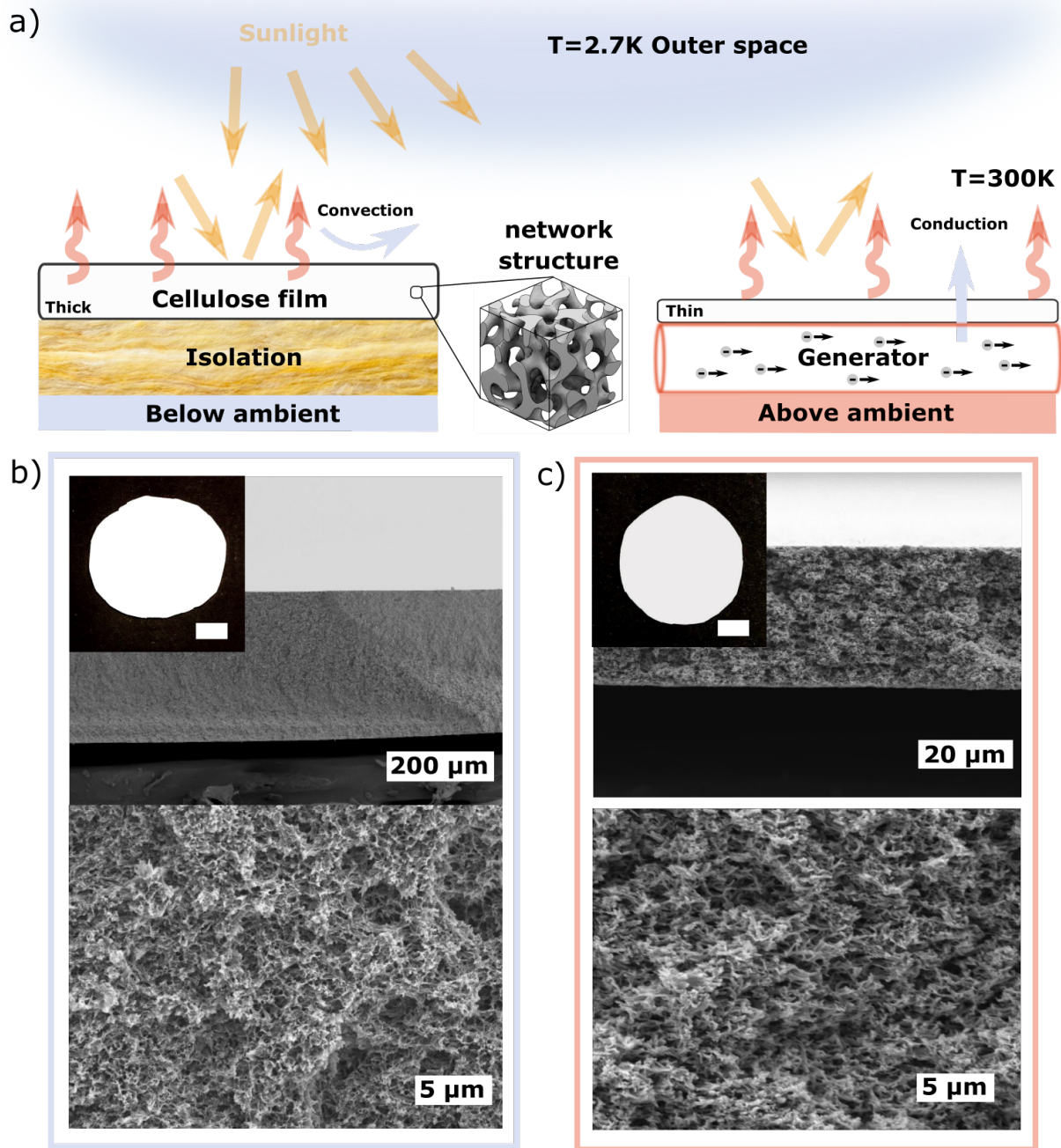


Figure 1: Highly scattering cellulose-based radiative cooling films (a) Illustration of radiative below-ambient (right) and above-ambient (left) cooling applications for a thick and a thin cellulose-based film. The inset is a schematic representation of the disordered network scattering structure. Sunlight (yellow) is reflected by the network structure of the film while thermal radiation (red) is emitted. The thin film enables improved heat conduction, favorable for above-ambient cooling applications while the thick one provides thermal insulation from conduction and convection. Electron microscopy images of (b) a thick ($\approx 300 \mu\text{m}$, filling fraction =48%) film and (c) a thin ($\approx 30 \mu\text{m}$, filling fraction =36%) film made of cellulose acetate (AC). Top: Cross-section image. Scale-bars are $200 \mu\text{m}$ and $20 \mu\text{m}$. Bottom: Zoom in. Scale-bars are $5 \mu\text{m}$ Inset: Macroscopic image of the films. Scale-bars are 1 cm .

our materials not only for protection and cooling in below-ambient applications but also for above-ambient cooling, i.e., heat generating substrates. The optical properties of the thick and thin films in the ultraviolet (UV) / visible (VIS) spectra are plotted in Figure 2b and Figure 2c, respectively. Both films show a low absorption down to 300 nm . It is noteworthy that both films have a remarkable high reflectance over the entire visible range and absorb only about 5% of the solar ir-

radiance, even in the case of the thin film (Table.1). The high reflectance in the visible is mainly caused by an optimal pore size distribution for Mie scattering with dominating sizes in the hundreds of nanometers (SI Fig S1). The low absorptance combined with the high-broadband reflectance over the whole solar spectrum makes these structures ideal for passive daytime radiative cooling.

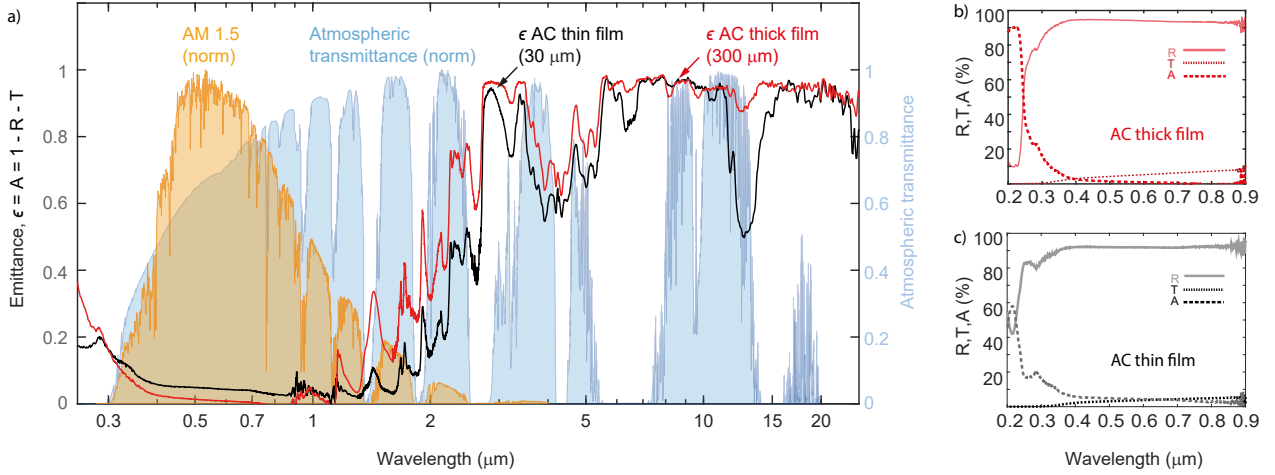


Figure 2: Optical properties of the cellulose-based radiative cooling films in the visible and mid-IR. (a) Comparison of the spectral emittance, ϵ , of the thin (black) and thick (red) cellulose based films measured from 0.25 to 25 μm . The spectra superimposed depict the normalised mid-latitude solar irradiance with an air mass coefficient (AM) of 1.5^[2] (orange) and atmospheric transmittance from MODTRAN^[7] (blue). Reflectance, transmittance and absorptance of (b) thick and (c) thin cellulose-based films in the UV-visible, from 0.2 to 0.9 μm

2.3 Radiative cooling performance

The radiative cooling of the cellulose-based films was evaluated by measuring the temperature reached by both films and comparing that with the ambient temperature. The films were attached to PT100-thermometers and the ambient temperature was measured using a Bresser PC weather station probe. A schematic illustration of the experimental test set-up and a cross section depicting the heat exchange processes are shown in Figure 3a and b. Details are given in the Experimental section 4. The thermal measurements were performed by exposing the experimental set-up to a clear sky throughout a 24-hour day/night cycle at the rooftop of a four-story building in Barcelona (Spain) in Autumn.

In Figure 3c-f, we plot the 24-hours cycle of the measured temperature of both the thin and the thick cellulose-based films along with the environmental conditions during the measurement. For reference, Fig. 3c shows the relative humidity (RH) (yellow curve, left axis) and the dew point (green curve, right axis), while Fig. 3d shows the solar irradiance (light-blue curve, left axis) and the wind speed (dark-blue curve, right axis). The time evolution of the temperature from both films and their corresponding temperature difference relative to the ambient are plotted in Fig. 3e and f, respectively. During daytime, both films maintained their temperatures below the ambient (Fig. 3b). Average below-ambient temperatures of 4.6 $^{\circ}\text{C}$ and 4.1 $^{\circ}\text{C}$ were measured for the thick and thin films, respectively, from 11:00 to 16:00, as plotted in Fig. 3e. During this period, the sky was clear, with a mean solar irradiance of 780 W/m^2 , a wind speed of 2.4 km/h (Fig. 3d) and an average relative humidity of 40 % (Fig. 3e). The maximum temperature difference with respect to the ambient was 5.3 $^{\circ}\text{C}$ and 4.9 $^{\circ}\text{C}$ around 11:30, for the thick and the thin film, respectively. These results indicate that the produced cellulose films are capable of

both preventing heating from diffuse solar irradiance and efficiently emitting heat as IR radiation. Finally, the maximal absolute temperature reduction from ambient was 5.5 $^{\circ}\text{C}$ and 5.2 $^{\circ}\text{C}$ measured just before noon (at 11:28) and at peak irradiance of 840 W/m^2 , for the thick and thin film, respectively. During the night, both films keep their temperatures below that of the ambient air, yet the temperature reduction compared to daytime is smaller, which suggests a decreased radiative cooling power. Average below-ambient temperatures values of 2.9 $^{\circ}\text{C}$ and 2.5 $^{\circ}\text{C}$ were recorded for the thick and the thin film, respectively (from 20:00 to 8:00, with average relative humidity of 86 % and wind speed of 0.5 km/h). The reduced capability of both film to keep temperatures below that of the ambient during the night is attributed to the higher relative humidity. The maximal temperature below ambient was 3.5 $^{\circ}\text{C}$ and 3.0 $^{\circ}\text{C}$ measured at 21:30, before the dew point temperature started to drop from 12 $^{\circ}\text{C}$.

To understand the measured thermal performance of the produced cellulose films, we calculate their daytime net cooling power as a function of the temperature difference between the radiative coolers and the ambient. For this purpose, their spectral emittances measured by FTIR are extrapolated for angles from 0 to 90 $^{\circ}$, assuming that they behave as Lambertian emitters. In Fig. 3g, we plot the directional spectral emittance of thin (top) and thick (bottom) films, over the IR transparency atmospheric window (from 8 - 14 μm). In Fig. 3h, we report the net cooling power estimated using the emittance values over the full mid-IR spectrum, considering a convection and conduction coefficient of $h = 11 \text{ W}/\text{m}^2\text{K}$ and $T_{amb} = 300 \text{ K}$. It is important to consider that to estimate the solar absorption, we only take into account diffuse sunlight, as the samples were characterized using a radiation shield. The atmospheric transmittance used to calculate the net cooling power was extracted using MOD-

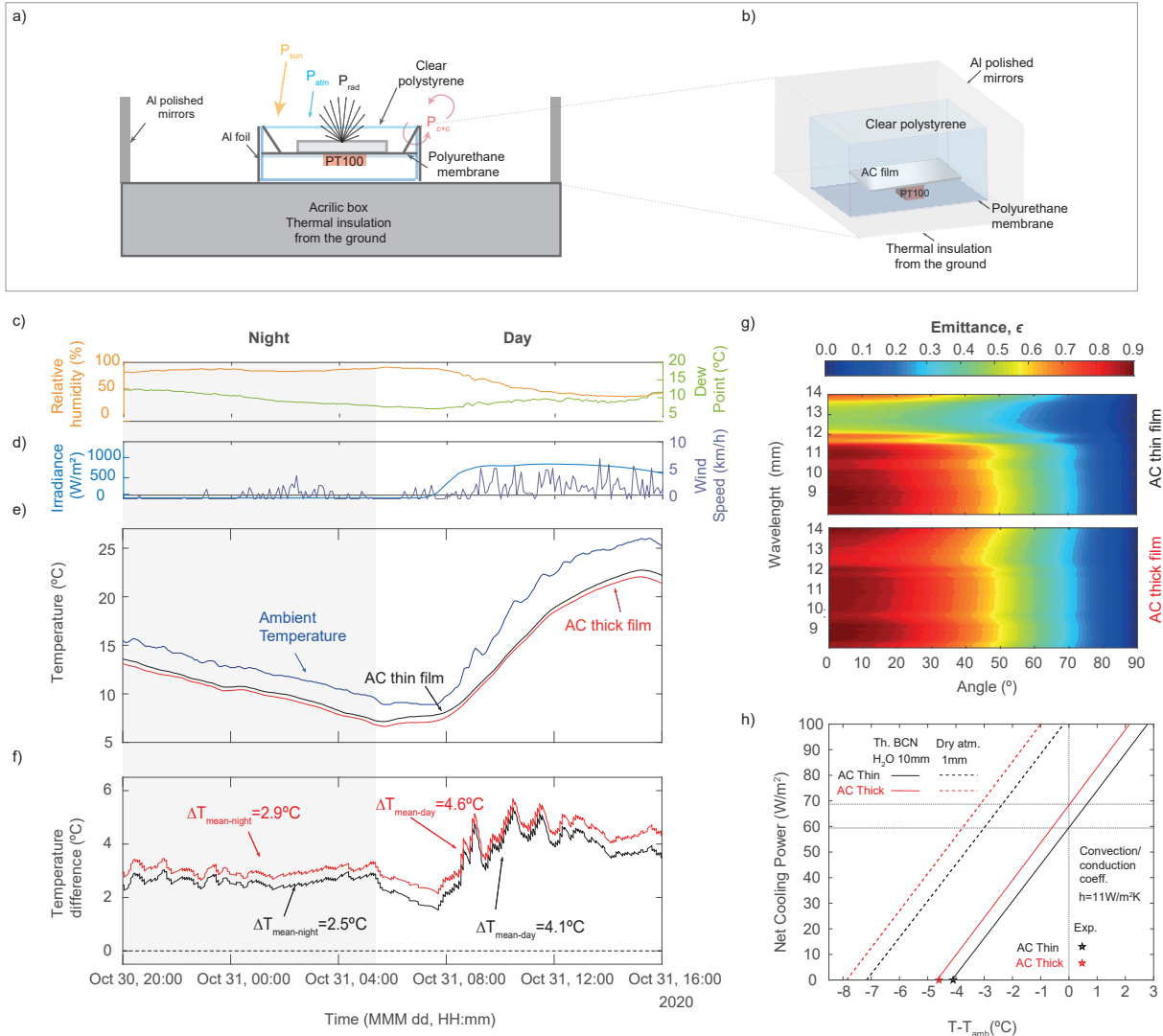


Figure 3: Testing the radiative cooling performance of cellulose-based films. (a) Cross section of the cellulose-based films in the test set-up insulated from the ground for continuous temperature measurements. (b) Schematics of the test setup. (c)-(g) Continuous temperature measurement for the thin and the thick AC films, along with the environmental conditions. (c) Relative humidity (RH) (yellow curve, left axis) and dew point (green curve, right axis). (d) Solar irradiance (blue curve, left axis) and wind speed (purple curve, right axis). (e) Measured cycle of temperature during 24 hours in a clear-sky day for the thin and the thick AC films. The ambient temperature is plotted in blue for reference. (f) Temperature difference between the ambient and the AC films. (g) Spectral directional emittance of thin (top) and thick (bottom) cellulose-acetate nanostructured films, assuming that they behave as Lambertian emitters. (h) Predicted net cooling power of the thin and thick cellulose-based films, for a conduction/convection coefficient of $11 \text{ W/m}^2\text{K}$, high atmospheric water vapor content (water column = 10 mm), representative of a Mediterranean location, such as Barcelona (continuous lines) and dry conditions (water column = 1 mm) (dashed lines).

TRAN,^[?] for vertical water vapor column conditions typical of Barcelona (water column = 10 mm) i.e high content of total gaseous water in a vertical column of atmosphere, compared to dry conditions (more details in Experimental Section. 4). The results are plotted in Fig. 3h, as black (thin film) and red (thick film) continuous lines. For the sake of comparison, we also report the theoretical net cooling power that can be achieved under dry atmospheric conditions (water column = 1 mm), as dashed lines in Fig. 3h. Finally, the average minimum temperature of the film achieved experimentally (in the steady-state regime) is shown in Fig. 3h, as open black (thin film) and red pentagons (thick film), respectively. This equilibrium temperature

is reached when the net cooling power becomes equal to zero, $T_r|_{P_{cool}=0}$. We use the difference between the emitter's temperature and the ambient at this point to characterise the below-ambient cooling performance of the surfaces (more details in Experimental Section. 4).

The black and red stars in Fig. 3h pinpoint the average minimum temperatures measured below ambient in the thick and thin films, $4.1 \text{ }^\circ\text{C}$ and $4.6 \text{ }^\circ\text{C}$, respectively, which match our predictions. The location of the experiment, close to Barcelona, is characterized by a Mediterranean climate, which exhibits higher water vapor content compared to other arid or high altitude locations under which several daytime radiative cooling experiments have been reported in the litera-

ture.^[?,?,?] The water vapor content in the atmosphere affects the radiative cooling efficiency which is reduced due to the absorption of the heat emitted from the film by the water vapor molecules in the lower atmosphere. We expect our films to reach average minimum temperatures of 7 °C (thin film) and 8 °C (thick film) below the ambient under dryer conditions (water column = 1 mm), as indicated in Fig. 3h by including a correction with dry conditions (dashed curves). For negligible convection and conduction (coefficient $h = 0$ W/m²K), our model predicts average minimum cooling temperatures of 37 °C (thin film) and 39 °C (thick film) relative to the ambient under dry atmospheric conditions. This requires to completely eliminate the non-radiative losses, as in previously reported works, e.g.^[?,?]

2.4 Towards scalable and sustainable radiative-cooling coatings

Hybrid cellulose-based materials have been designed recently to optimize their optical and thermal performance for radiative cooling in either the VIS or mid-IR spectral regimes.^[?,?,?,?] In these materials, cellulose is serving as a matrix and/or scattering material to optimize the optical properties in the visible but the IR emission is obtained by adding thermal-emitting polar materials such as Al₂O₃, TiO₂ and SiO₂ nano or microspheres. Here, we engineer cellulose as an all-in-one radiative-cooling material by obtaining thick and thin films via phase separation with optimized optical and thermal properties simultaneously. Our material has been additionally tested for radiation durability using a Bandol wheel instrument in which the films were irradiated for 100 hours, which is equivalent to 50 - 100 years of indoor illumination conditions, or about 6 months of direct outdoor sun exposure. The color change (ΔE_{00}) is a useful number for assessing subtle changes. For reference, humans in general wont visually notice a difference until ΔE_{00} reaches about 2. The ΔE_{00} of the thin and thick AC films after Bandol wheel test is only 0.88 and 0.16, respectively.

A comparison of the physical properties relevant to radiative cooling between recently reported cellulose-based materials and our films is shown in Table 1. Chen et al.^[?] and Li et al.^[?] were the first to report on cellulose-based structural materials for radiative cooling with excellent mechanical properties for architectural applications. These materials were developed for building applications and therefore their dimensions are, at least, one order of magnitude greater than the films here reported. Interestingly, the highly scattering AC films absorb a much lower fraction of solar irradiance, as cellulose acetate has better performance in the UV spectral range compared to pure cellulose. The heating power resulting from solar absorption is ≈ 47 and 45 W/m² for the thin and the thick films, respectively, compared to 64 and 70 W/m² for the thicker materials from refs.^[?] and.^[?] This reduction represents

a gain in net cooling power of at least 17 W/m², despite the fact that our films are two and one order of magnitude thinner than the reported structural materials. Very recently, Gamage et al.,^[?] demonstrated reflective and transparent radiative coolers based on cellulose derivatives manufactured via electrospinning and casting. Our 300 μm -thick films exhibit comparable optical properties in the visible and mid-IR with respect to their 275 μm -thick film. In contrast, our 30 μm -thin films achieve high reflectance across the whole solar spectrum and strong average IRAW emittance (Table 1), despite their small thickness, while their thinnest reported film (60 μm) is partially transparent in both wavelength ranges. This highlights the efficient broadband light scattering that we achieve in such thin films with the network scattering nanostructure.

3 Conclusion

In conclusion, we have obtained efficient radiative-cooling films using only an abundant and biodegradable cellulose-derivative. Our scalable-production process is based on air-drying, which does not require any sophisticated nanostructuring neither the incorporation of dielectric particles that act as optical scatterers. The cellulose-acetate films have a disordered network morphology enhancing the reflectance across the whole solar spectrum ($\lambda \approx 0.3 - 2.5 \mu\text{m}$), which results in minimal absorption of ≈ 5 % of the solar irradiance (Table 1). At the same time, the produced films exhibit strong mid-IR emittance, in particular within the IR atmospheric transparency window. In addition, we demonstrated that by tuning the thickness, different optical and thermal properties can be achieved: The thick films have stronger emittance in the IR atmospheric transparency window ($\epsilon_{IRAW} \approx 93.6$ %) and are suitable for sub-ambient applications, where conduction and convection minimization is required to cool down an underlying substrate. The thin films exhibit slightly lower $\epsilon_{IRAW} \approx 87.9$ % and modest transmittance $\epsilon_{IRAW} \approx 7.5$ % in the IR atmospheric transparency window. Their reduced thickness (lower thermal resistance), makes them ideal for above-ambient applications, where the underlying material produces heat and convective/conductive heat transfer become beneficial for the net cooling (See the Supplementary Information). All the thermal performances of the cellulose-based radiative coolers were assessed during field tests. The produced thin and thick cellulose films reached up to ≈ 5.0 °C and ≈ 5.2 °C below ambient temperature, when convection/conduction losses and direct solar irradiance were minimized. Under dryer conditions (water column = 1 mm), we estimate that our films can reach average minimum temperatures of 7 °C (thin film) and 8 °C (thick film) below the ambient. We, therefore, believe that our work provides a novel all-in-one large-scale cost-efficient radiative cooling material fabricated using solely sustainable cellulose-based compounds, that are adaptable to different types of cooling

	Thickness [μm]	Solar abs. power [W/m^2] (0.3-2.5 μm)	Solar abs. [%] (0.3-2.5 μm)	ϵ_{IRAW} [%] (8-13 μm)	T_{IRAW} [%] (8-13 μm)	ϵ_{mIR} [%] (2.5-25 μm)
AC thin film	30.0	46.7	5.2	87.9	7.5	78.2
AC thick film	300.0	44.8	5.0	93.6	1.3	87.1
Hybrid structural material ^[?]	4000.0	64.2	7.2	91.1	-	85.9
Structural material ^[?]	≥ 10000.0	70.4	7.8	91.7	-	86.1

Table 1: Comparison of the the absorptance in the UV-VIS or mIR spectral ranges for recently reported cellulose-based materials for radiative cooling. The symbol "-" refers to data not available.

applications.

4 Experimental Section

Materials. Cellulose acetate -Acetylcellulose- (AC) with relative molecular mass $\simeq 29000$) and acetone were purchased from Sigma Aldrich. **Preparation of cellulose acetate thin films.** The films were prepared via air drying in a petri dish from the same cellulose acetate solutions containing acetone, water and cellulose acetate powder. About 3% wt. cellulose acetate was added to an acetone-water mixture solution with 5% wt. of water. The suspension was stirred vigorously to completely dissolve the cellulose acetate powder. The final solution contains 3% cellulose acetate. Thin white films were formed by slowly drying the cellulose acetate-acetone-water mixture solution in a glass petri dish. **Preparation of cellulose acetate thick films.** Cellulose acetate powder was added into pure acetone under vigorously stirring till its weight percentage was 24% wt. The glue-like solution was transferred into a glass petri dish which was soaked in water to form a white film and dried at 60 °C in a vacuum oven. The thickness of the film was determined by the total volume of the solution poured into a petri dish with a diameter of 4.7 cm. Typically, 1 ml and 2 ml solutions were used for thin and thick films, respectively.

Characterization of cellulose-based white films by SEM. The cross-section of each film was measured by scanning-electron microscope (SEM) with a Mira3 system (TESCAN) operated at 5 kV and a working distance of about 6 mm. To prepare specimens, the films were frozen in liquid nitrogen and then cracked. The samples were mounted on aluminum stubs using conductive carbon tape and coated with a layer of platinum (10 nm in thickness) by a sputter coater (Quorum Q150T ES). The thickness of each film was determined from the SEM images of their cross-sections.

Optical characterization of cellulose-based white films by UV-VIS spectroscopy. The optical properties of the films in the ultraviolet (UV) / visible (VIS) spectra where measured from 300 to 800 nm using a Cary 4000 spectrometer equipped with an integrating sphere.

Characterization of cellulose-based white films by FT-IR. The emittance of the films in the mid-IR was measured by Fourier-transform infrared

(FT-IR) spectroscopy, using a gold integrating sphere to collect the near-normal reflected, transmitted and scattered light over a solid angle of 2π sr, from wavelength of 0.9 μm to 25 μm . A direct approach to obtain the emittance is by measuring the absorptance A , the fraction of radiation absorbed by the films. We assume that the directional spectral emittance is equal to the directional spectral absorptance, $\epsilon(\lambda, \theta, \phi) = A(\lambda, \theta, \phi)$ under thermodynamic equilibrium, according to the Kirchhoff's law of thermal radiation.^[?] The absorptance is given directly by taking the difference of the measured reflectance and transmittance of the samples in the infrared spectrum from unity ($A = 1 - R - T$).

Atmospheric transmittance and net cooling power calculations The atmospheric transmittance used in the net cooling power calculation was obtained using MODTRAN [®] .^[?] MODTRAN (MODerate resolution atmospheric TRANsmission) is a computer code used to predict atmospheric spectral transmittances and radiances over the ultraviolet through long wavelength infrared spectral regime. The atmosphere model considered a mid latitude region during summer, which corresponds to a vertical water vapor column conditions typical of Barcelona i.e high content of total gaseous water in a vertical column of atmosphere, compared to dry conditions. The net cooling power calculations were performed following the procedure described in ref.^[?]

Continuous passive radiative cooling measurements of cellulose-based films. During the experiment, the parasitic conduction and convection were minimized. To reduce these heat losses, the films were placed on a low-thermal conductivity membrane suspended inside a poly-methacrylate box used as a sample holder and covered with aluminium foil to minimize heat gain due to solar absorption. The top of the poly-methacrylate box was covered with a low-density polyethylene film that is transparent in the relevant wavelengths, in order to reduce convection through the top. Further details are given in the Supplementary Information. The poly-methacrylate boxes used as sample holders were placed on a acrylic structure, of 70 cm of height, that thermally insulates the system from the ground. The structure is also covered with aluminum foil to reflect the visible light and minimize parasitic heating (Fig.3b). Polished aluminum sheets were placed as solar radiation shields, that help also to minimize the lateral convection and reflect outgoing IR radiation. The polished aluminum sheets are mainly used to avoid parasitic heating due to direct solar irra-

diance, as radiation shields, used following the experimental procedure reported by Chen et al.^[7]

Acknowledgements

This work was supported by the BBSRC David Phillips fellowship [BB/K014617/1] and the Horizon 2020 Framework Programme Marie Curie Individual Fellowships (793643-MFCPF), ERC SeSaME ERC2014STG H2020 639088, the PoC 963872, Cellunan, and the Isaac Newton Trust (SNSF3) and the Philip Leverhulme Prize (PLP-2019-271).

The European Unions Horizon 2020 Research and Innovation Program partly funded this research (Marie Skłodowska-Curie Actions Grant No. 665919 that supported J.J.F and the project FLEXPOL Grant. No. 721062 that supported G.L.W). Moreover, the research received funds from the Spanish Minister of Science, Innovation and Universities via the Severo Ochoa Program (Grant No. SEV-2017-0706) that supports ICN2, and the projects PGC2018-101743-B-I00 (SIP) and RTI2018-093921-A-C44 (SMOOTH), as well as by the

CERCA Program/Generalitat de Catalunya. L.S. acknowledges the support of the Swiss National Science Foundation under project 40B1-0_198708. P.D.G gratefully acknowledges the support the Ramon y Cajal fellowship (RYC-2015-18124). L.S is grateful to Johannes S. Haataja for providing the 3D network graphic in Fig. 1. J.J.F. is grateful to A. El-Sachat and P. Xiao for thermal conductivity measurements and gold deposition, respectively.

Authors contributions

J.J.F, H.Y. and L.S. contributed equally to this work. S.V. and P.D.G conceived the idea and the project, and supervised the work. H.Y. fabricated the samples and performed optical measurements for material choice. L.S. analysed the optical, the thickness and morphology results. J.J.F. performed the UVVIS and FTIR spectroscopy, thermal and radiative cooling measurements and analysed of the optical and thermal results. G.L.W. and J.J.F calculated the net cooling power. J.J.F., P.D.G., L.S and H.Y wrote the manuscript with all author's contributions